Mat. Res. Soc. Symp. Proc. Vol. 674 © 2001 Materials Research Society

Multilevel Magnetoresistance in a Structure Consisting of two spin-valves

Kebin Li, Yihong Wu[1], Jinjun Qiu, Guchang Han, Zaibing Guo, and Towchong Chong
Data Storage Institute, DSI Building, 5 Engineering Drive 1, Singapore 117608
[1]Department of Electrical and Computer Engineering, National University of Singapore, 10 Kent Ridge Crescent, Singapore 119260

ABSTRACT

The magnetic and electrical properties as well as the structural characteristics have been studied on a series of samples with structure substrate (Sub)/SV(1)/$Al_2O_3$5nm/SV(2). Here, SV(1) is either CoFe/IrMn based spin-valve (SV) such as Ta5/NiFe2/IrMn8/CoFe2/Cu2.6/CoFe2/Ta5 (thicknesses are in nanometers) bottom SV or Ta5/NiFe2/CoFe1.5/Cu2.6/CoFe2/FeMn10/Ta5 top SV and SV(2) is Ta5/NiFe2/CoFe1.5(or 2)/Cu2.6/CoFe2/IrMn8/Ta5 top SV. SV(1) and SV(2) in the structure are decoupled by a Al_2O_3 layer with 5nm in the magnetic properties, however, they are in parallel connection in the electrical properties. In a sample with structure Sub/Ta5/NiFe2/IrMn8/CoFe2/Cu2.6/CoFe2/Ta5 /$Al_2O_3$5/Ta5/NiFe2/CoFe2/Cu2.6/CoFe2/IrMn8/Ta5, five magnetoresistance states which are related to five magnetization states have been observed after the sample was annealed at T=220 °C with a field strength of 1T under high vacuum because of different interlayer coupling fields (H_{int}) in the top and bottom CoFe/IrMn based SVs (H_{int} is about 12.21 Oe in the top CoFe/IrMn SV and 29.3 Oe in the bottom CoFe/IrMn based SV). In a sample with structure Sub/Ta5/NiFe2/CoFe1.5/Cu2.6/CoFe2/FeMn10/Ta5/$Al_2O_3$5/Ta5/NiFe2/CoFe1.5/Cu2.6/CoFe2 /IrMn8/Ta5, since the blocking temperature of the CoFe/FeMn based SV (T_b is about 150 °C) is lower than that of CoFe/IrMn based SV (T_b is about 230 °C), the spins can be easily engineered and therefore various magnetoresistance states can be obtained when the sample is magnetically annealed at different temperatures in a proper annealing sequence. By properly selecting materials and controlling the magnetically annealing conditions, multilevel giant magnetoresistance (MR) magnetic random access memory (MRAM) cell can be realized, which will significantly improve the MRAM data storage density without increasing any additional processing complexity.

INTRODUCTION

Multiple value storage is considered as a promising technique for increasing the storage density of magnetic random access memories (MRAMs). In order to implement this technique, one must first identify a suitable cell structure featuring a multi-step response in the magnetoresistance (MR) versus magnetic field curve. Such a structure has been once reported in a NiFe/Cu/NiFeCo/Cu/NiFeCo/Cu/Co pseudo-spin-valve (PSV).[1] However, the MR ratio of the PSV is rather small which may limit its applications in large scale MRAMs. In this paper, we report a new structure that consists of two electrically isolated and magnetically decoupled CoFe/IrMn spin-valves or CoFe/FeMn spin-valves. Multiple distinctive steps associated with different magnetization states have been successfully observed in the MR response curves. The potential application of this structure in multiple value MRAMs will be discussed.

EXPERIMENTAL DETAILS

The sample was fabricated by using a multiple chamber ultra-high vacuum (UHV) sputtering system operating at a base pressure of 5×10^{-10} Torr. The use of inductively coupled plasma makes it possible to deposit the thin films at a low process pressure (about 1mTorr). The sample was deposited on a 4" round Si(100) substrate coated with a 100nm-thick thermally oxidized SiO_2 layer. A typical layer structure is as follows: Ta5/NiFe2/IrMn8/CoFe2/Cu2.6/CoFe2/Ta5/ Al_2O_35/Ta5/NiFe2/CoFe2/Cu2.6/CoFe2/IrMn8/Ta5. The UHV sputtering system was configured with four processing chambers which makes it possible to deposit the whole structure without breaking the vacuum. During deposition of the magnetic layers, a magnetic field with a strength of 100 Oe is applied along a certain direction parallel to the film surface. The 5nm-thick Al_2O_3 layer was thick enough to magnetically decouple and electrically isolate the bottom and the top spin-valves, though the two would be electrically connected during the magnetoresistance measurement due to the penetration of the probes vertically through the spin-valve structure. The magnetic properties and MR curves were measured with a vibrating sample magnetometer equipped with a MR measurement fixture. Annealing was conducted in a commercial high-vacuum magnetic annealing oven at a base pressure lower than 8×10^{-7} Torr for 2 hours at 220 °C with a field strength of 10 kOe. The crystal structure of SVs was characterized by XRD.

RESULTS and DISCUSSIONS

The resistance versus magnetic field (R-H) and magnetization versus magnetic field (M-H) were measured on annealed SVs, (a)Sub/Ta5/NiFe2/CoFe2/Cu2.6/CoFe2/Ta5/Al_2O_3 (SV1),
(b) Sub/$Al_2O_3$5/Ta5/NiFe2/IrMn8/CoFe2/Cu2.6/CoFe2/Ta5 (SV2),
(c) Sub/Ta5/NiFe2/CoFe1.5 /Cu2.6/CoFe2/FeMn10/Ta5/Al_2O_3 (SV3),
(d) Sub/$Al_2O_3$5/Ta5/NiFe2/CoFe1.5/Cu2.6/CoFe2 /IrMn8/Ta5 (SV4),
(e) Sub/$Al_2O_3$5/Ta5/NiFe2/CoFe2/IrMn8/CoFe2/Cu2.6/CoFe1.5/NiFe2/Ta5 (SV5), and,
(f) Sub/Ta5/NiFe2/FeMn10/CoFe2/Cu2.6/CoFe1.5/NiFe2/Ta5 (SV6). Due to limit of paper length, only four of them are shown in Fig.1. But the interlayer coupling field between the free FM layer and the pinned FM layer across the spacer layer H_{int} and a coercivity field H_c of the free layer , which are defined as in Ref.[2], exchange coupling field H_{ex} as well as MR ratio for these six single SVs are summarized in Table(1). The overall properties of these single SVs are comparable to that published [3-7]. It is worth of noting that for FeMn-based SV, H_{ex} is about 490 Oe for top type and 500 Oe for bottom type, corresponding to the exchange coupling energy J_k~0.13 erg/cm^2 (M_s=1300emu/cm^3 is assumed). Such high exchange coupling energy observed in the FeMn/CoFe SV should be attributed to the better (111) texture structure of γ-FeMn crystallite formed in the SV as shown in Fig.2(a). From XRD results, the (111) texture structure of γ-FeMn crystallite was overlapped with NiFe(111)/CoFe(111), indicating the lattice mismatch between them is very small. Both top SV and bottom SV show that (111) texture structure of γ-FeMn was well formed, there is no distinct difference between them. The XRD patterns of a single top IrMn SV, a single bottom IrMn SV and a composite SV (CSV1) are shown in Fig.2(b) after magnetically annealed.

Figure 3(a) shows the M-H loop measured on an electrically isolated and magnetically decoupled dual SV with structure Sub/Ta5/NiFe2/IrMn8/CoFe2/Cu2.6/CoFe2/Ta5/$Al_2O_3$5/

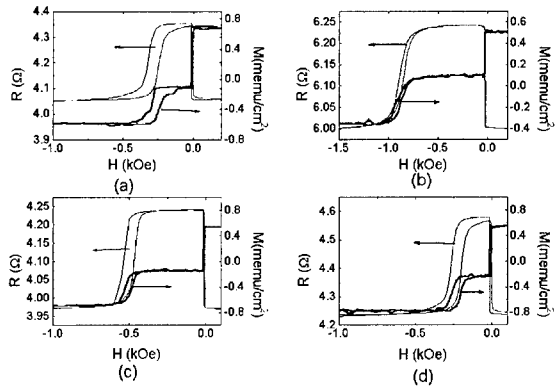

Fig.1 R-H and M-H curves for magnetically annealed (a) SV1, (b) SV2, (c) SV3, and (d) SV4

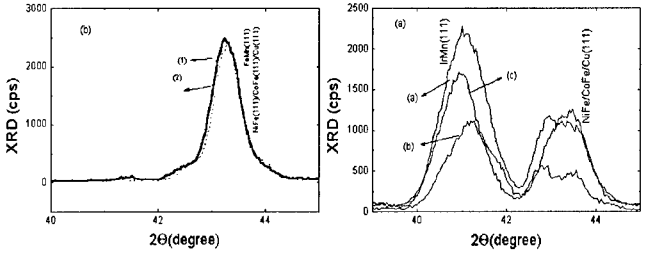

Fig.2 (a) XRD patterns of annealed (1) Sub/Ta5/NiFe2/CoFe1.5/Cu2.6/CoFe2/FeMn10/Ta5, and, (2) Sub/Ta5/NiFe2/FeMn10/CoFe2/Cu2.6/CoFe1.5/NiFe2/Ta5 SVs. The (111) texture structure of γ-FeMn is overlapped with NiFe(111)/CoFe(111)/Cu(111). There is no distinct difference between the top CoFe/FeMn and bottom FeMn/CoFe. Fig.2(b) XRD pattern of (a) a bottom spin-valve, (b) a top spin-valve, and (c) a new structure consists of a top SV and a bottom SV separated by a 5nm-thick Al_2O_3 layer after magnetically annealed.

Ta5/NiFe2/CoFe2/Cu2.6/CoFe2/IrMn8/Ta5 (termed as CSV1). When an applied magnetic field is applied along the pinning direction, the magnetizations of the free layer and the pinned layer in the CSV1 are parallel to the sweeping field axis. As the field strength increases in the opposite direction, the free layer in the top part changes its magnetization direction at -12.2 Oe and the total magnetizations drop to a lower state. The magnetizations drop to another lower state when the free layer of the bottom part starts to change its magnetization direction at -29.36 Oe. After that, it keeps a constant until the magnetic field increases to about -260 Oe at which the pinned layer of the top part changes its magnetization direction, too. Hence the total magnetizations become negative. When the field strength increases to about 865 Oe, the magnetizations jump to a higher step and become saturation. Five different magnetic states are schematically illustrated in the figure. The thickness of the arrow indicates the strength of the magnetic field that is required to flip the magnetization direction of the ferromagnetic layers.

Table (1) Some basic parameters obtained from R-H and M-H curves measured on several single IrMn-based SVs and FeMn-based SVs.

	H_{int}(Oe)	H_c(Oe)	H_{ex}(Oe)	M_s(NiFe)(emu/cm^3)	M_s(CoFe) (emu/cm^3)	MR(%)
SV3	12.0	3.0	500	725±50	1300±70	6.75
SV4	8.7	6.3	234	780±50	1203±70	8.16
SV5	24.4	2.9	764	760±50	1112±70	4.74
SV6	30.7	2.2	490	739±50	1070±70	3.94
SV1	10.1	2.8	278	785±50	1179±70	7.55
SV2	27.0	2.1	896	200±50	1013±70	4.09

As it is expected, there are five magnetoresistive states observed in the MR curve shown in Fig. 3(b). The resistance (R) is at the lowest level when the magnetization is at state one. At the second magnetization-state, R increases to a higher step because the top part is at the highest resistance-state due to the antiparallel alignment of the magnetization in the free layer and the pinned layer. At the third magnetization-state, both the top and bottom parts are at the highest resistance-state, so R reaches to the highest step. At the fourth magnetization-state, the total resistance drops to a lower step because the resistance in the top part is at the lowest level due to the parallel alignment of the magnetizations in the free and pinned ferromagnetic layers. And at the fifth magnetization-state, the total resistance is at the lowest state again.

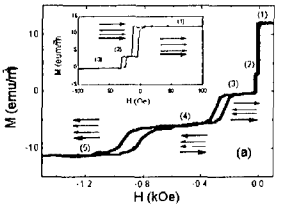

Fig.3(a) M-H loop for CSV1, five magnetization states are clearly shown in the figure. The arrows indicate the spin direction. The insert is the minor M-H loop

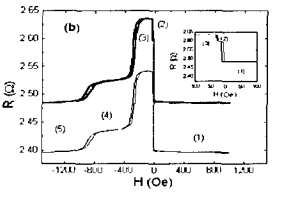

Fig.3(b) MR curve of CSV1. The thinner line are fitted by using a parallel connection of the resistance of the top SV and that of the bottom SV shown in Fig.1 (a), and (b).

The dotted lines in the Fig.3(b) was fitted by using a simple parallel connection of the resistance of the top SV and that of the bottom SV shown in Fig.1. All the features observed in the MR curve of the CSV1 are perfectly reproduced except that the fitted resistance is smaller than the measured data. The discrepance in resistance between them comes mainly from one addition 5 nm Ta layer used in the single top spin-valve and one addition Al_2O_3 layer used in the single bottom structure. The good agreement between the fitted and measured data suggests that the unique magnetoresistance characteristics observed in CSV1 should result from the simply parallel connection of two SVs used in the electrically isolated and magnetically decoupled dual SV.

Multiple steps have also been observed in the magnetoresistance response curve of SV with structure Ta5/NiFe2/CoFe1.5/Cu2.6/CoFe2/FeMn10/Ta5/$Al_2O_3$5/Ta5/NiFe2/CoFe1.5/Cu2.6 /CoFe2/IrMnIrMn8/Ta5 (termed as CSV2). Since the blocking temperature of the CoFe/FeMn SV is different from that of IrMn/CoFe SV[5,8], the exchange coupling orientation of

CoFe2/FeMn10 and CoFe2/IrMn8 can be either set in the same direction or in the opposite direction. Fig.4 shows the MR curves of CSV2 when the exchange coupling orientation of CoFe/FeMn and CoFe/IrMn was set in the same direction. The dotted line shown in the Fig.4 was fitted by a simple parallel connection of R-H curves of top CoFe/IrMn and CoFe/FeMn SVs shown in Fig.1 (c) and (d). Again, the electrical properties of CSV2 are the electrical properties of two SVs in parallel connection.

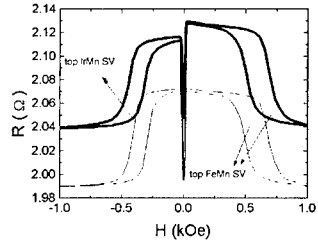

Fig.4 R-H curve for CSV2 when the exchange coupling orientation of CoFe/FeMn and CoFe/IrMn was set in the same direction. The dotted line shown in the Fig.4 was fitted by a simple parallel connection of R-H curves of top CoFe/IrMn and CoFe/FeMn SVs shown in Fig.1 (c) and (d).

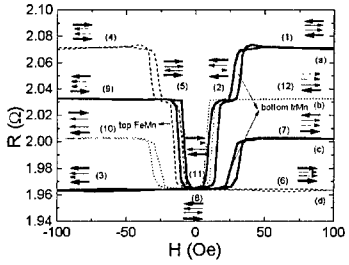

Fig.5 Minor R-H loops of an annealed composite CSV3. Twelve magnetization states are illustrated in the figure, which are corresponding to four different magnetoresistance states (a), (b), (c) and (d). The arrows represent the magnetization of each FM layers in the structure.

Multiple magnetoresistance levels were also observed in a composite SV with structure Sub/Ta5/NiFe2/CoFe2/IrMn8/CoFe2/Cu2.6/CoFe1.5/NiFe2/Ta5/$Al_2O_3$5/Ta5/NiFe2/CoFe1.5/Cu 2.6/CoFe2/FeMn10/Ta5 (termed as CSV3). The minor R-H loops of annealed CSV3 are shown in Fig5. The thicker solid line is corresponding to the minor R-H loop of CSV3 when the exchange coupling orientation of two SVs were set at the same direction (along the negative direction of the external magnetic field axis). The thinner solid line is corresponding to the minor R-H loop of CSV3 when the exchange coupling orientation of two SVs were set in the opposite direction. Where, the exchange coupling orientation of the top CoFe/FeMn was set along the positive direction of the external magnetic field axis, while the exchange coupling orientation of the bottom IrMn/CoFe was set along the negative direction. The thicker dotted line is corresponding to the minor R-H loop when the exchange coupling orientation of two SVs were set along the positive direction of the external magnetic field axis. The thinner dotted line is corresponding to the minor R-H loop of CSV3 when the exchange coupling orientation of the top CoFe/FeMn was set along the negative direction of the external magnetic field axis, while it was set along the positive direction in the bottom IrMn/CoFe SV. Although there are four different magnetoresistance levels shown in Fig.5, twelve different magnetization states are indicated in the figure, which are illustrated in the Fig.5, too. In fact, magnetization states (1) and (4) in which the magnetization of the free FM and pinned FM layers are in anti-parallel alignment both in the bottom IrMn/CoFe SV and top CoFe/FeMn SV, are corresponding to the same magnetoresistance state (a). Magnetization states (2), (5), (9) and (12), where the magnetizations of the free FM and pinned FM layers are in parallel alignment in the bottom IrMn/CoFe SV while they are in anti-parallel alignment in the top CoFe/FeMn SV, are corresponding to the

same magnetoresistance state (b). Magnetization states (7) and (10) in which the magnetizations of the free FM and pinned FM layers are in anti-parallel alignment in the bottom IrMn/CoFe SV while they are in parallel alignment in the top CoFe/FeMn SV, are corresponding to the magnetoresistance state (c). Magnetization states (3), (6), (8), and (11), in which the magnetizations of the free FM and pinned FM layers are in parallel alignment both in the top CoFe/FeMn SV and bottom IrMn/CoFe SV, are corresponding to the same magnetoresistance state (d).

These twelve magnetization states illustrated in Fig.5 can be individually distinguished based on the field dependence of the resistance. Hence, in principle, four magnetization states can be used as information storage if only two free FM layers in the composite spin-valve are used as storage layers. One can define the magnetization state (1) as "11" where the magnetization of both free FM layers are in parallel alignment along the positive direction. One can also define the state (2) as "01" where the magnetization of the free FM layer in the bottom IrMn/CoFe spin-valve is parallel to the negative direction while the magnetization of the free FM layer in the top FeMn/CoFe spin-valve is parallel to the positive direction. And so on so forth, two bits with four states can be finally stored and read out in one storage cell. If three FM layers are used as information storage, in principle, three bits with eight states can be stored and read out in one storage cell.

CONCLUSIONS

In summary, multiple magnetoresistance states have been successfully demonstrated in an electrically isolated and magnetically decoupled dual spin-valve structure. By properly choosing the FM and AFM materials used in the new structure, the spins of the free FM and pinned FM layers can be engineered as desired. Such kind of new structure is expected to be used as a MRAM cell in which multiple magnetization states can be stored and read out, hence the data storage density will be significantly improved without increasing any additional processing complexity.

Acknowledgement:

The authors would like to thank Joon Fatt Chong and Phyllis Tan for the XRD measurements.

REFERENCES

[1] Won-Cheol Jeong, Byung-Il Lee, and Seung-Ki Joo, J. Appl. Phys. **85**, 4782(1999)
[2] K.-S. Moon, R.E. Fontana, Jr., and S. S. P. Parkin, Appl. Phys. Lett. **74**, 3690 (1999)
[3] Hiromi Niu Fuke, Kazuhiro Saito, Yuzo Kamiguchi, Hitoshi Iwasaki, and Masashi Sahashi, J. Appl. Phys. **81**, 4004(1997)
[4] Geoff Anderson, Yiming Huai, and Lena Miloslawsky, J. Appl. Phys. **87**, 6989(2000)
[5] A. J. Devasahayam, P. J. Sides, and M.H.Kryder, J. Appl. Phys. **83**, 7216(1998)
[6] S. -F. Cheng and P. Lubitz, J. Appl. Phys. **87**, 4927(2000)
[7] Hiromi N. Fuke, Kazuhiro Saito, Masatoshi Yoshikawa, Hitoshi Iwasaki, and Masashi Sahashi, Appl. Phys. Lett. **75**, 3680(1999)
[8] G. Choe and S. Gupta, Appl.Phys.Lett. **70**, 1766(1997)